

# **Heterodyne diffracted beam photonic Doppler velocimeter (DPDV) for measurement of transverse and normal particle velocities in pressure-shear plate impact experiments**

Michael Mello, Christian Kettenbeil, Moriah Bischann, and Guruswami Ravichandran

Citation: [AIP Conference Proceedings](#) **1979**, 160017 (2018); doi: 10.1063/1.5045016

View online: <https://doi.org/10.1063/1.5045016>

View Table of Contents: <http://aip.scitation.org/toc/apc/1979/1>

Published by the [American Institute of Physics](#)

---

---

# Heterodyne Diffracted Beam Photonic Doppler Velocimeter (DPDV) for Measurement of Transverse and Normal Particle Velocities in Pressure-Shear Plate Impact Experiments

Michael Mello<sup>1,a)</sup>, Christian Kettenbeil<sup>1,b)</sup>, Moriah Bischann<sup>1,c)</sup> and Guruswami Ravichandran<sup>1,d)</sup>

<sup>1</sup>California Institute of Technology, M/C 104-44, 1200 E California Blvd Pasadena, CA 91125, USA

<sup>a)</sup> Corresponding author: mello@caltech.edu

<sup>b)</sup> ckb@caltech.edu

<sup>c)</sup> mbischan@caltech.edu

<sup>d)</sup> ravi@caltech.edu

**Abstract.** Pressure-shear plate impact (PSPI) experiments have traditionally relied on free space beam interferometers such as the transverse displacement interferometer (TDI) and normal displacement interferometer (NDI) or normal velocity interferometer (NVI), to measure transverse and normal velocities at the rear surface of the target plate [1]. Alternative interferometer schemes feature a dual beam VISAR arrangement [2] and a recently developed all fiber-optic TDI-NDI/PDV configuration [3]. Here, we present a heterodyne diffracted beam PDV (DPDV) which interferes a pair of symmetrically diffracted 1<sup>st</sup> order beams produced by a thin, specular, metallic grating deposited on the rear surface of the target plate. Each beam is collected by a fiber-optic probe and directed to interfere with a reference beam of a slightly increased wavelength to create an upshifted carrier signal frequency at zero particle velocity. Signal frequencies are extracted from the two fringe records using a moving-window DFT algorithm and then linearly combined in a post processing step to decouple the normal and transverse velocities. The 0<sup>th</sup> order beam can also be interfered in a heterodyne PDV to obtain an additional independent measurement of the normal particle velocity [4]. An overview of the DPDV configuration is presented along with a derivation of the interferometer sensitivities to transverse and normal particle velocities. Results from a normal impact experiment conducted on y-cut  $\alpha$ -quartz are presented as experimental validation.

## INTRODUCTION

The present paper addresses the development, and experimental validation of a heterodyne diffracted beam PDV (DPDV) system for the measurement of normal and transverse particle velocity components in pressure-shear plate impact (PSPI) experiments. Three fiber-optic probes collect the reflected (0<sup>th</sup> order) beam and symmetric  $\pm 1^{\text{st}}$  order beams produced by a 400 lines/mm metallic diffraction grating deposited onto the polished rear surface of the target plate. Fiber-optic probes are designed to collect light even as the diffracted beams are slightly rotated due to tilt between impact faces and de-centered due to the normal displacement of the target plate rear surface. The 0<sup>th</sup> and  $\pm 1^{\text{st}}$  order beams are each passed through a fiber-optic circulator and combined with a reference beam of a slightly higher wavelength to create a heterodyne signal with an upshifted carrier frequency at zero particle velocity. The frequency content encoded within the recorded DPDV fringe records corresponds to a scaled linear combination (sum or difference) of the normal and transverse particle velocity components. A moving-window discrete Fourier transform (DFT) algorithm is applied to extract the DPDV signal frequencies  $f^+(t)$  and  $f^-(t)$ , which also contains the constant user-selected carrier frequency. Normal and transverse particle velocity components are subsequently decoupled through addition or subtraction and appropriate scaling of the extracted signal frequencies. The normally reflected (0<sup>th</sup> order) beam can also be interfered in a heterodyne PDV arrangement to obtain an additional independent measurement of the normal particle velocity. The fiber-optic DPDV system has been configured with a powder gun capable of achieving impact velocities of 1.8 km/s and will enable future PSPI shock wave experiments designed to investigate strength and failure properties of novel materials at shear strain rates approaching  $\dot{\gamma} = 10^8 \text{ s}^{-1}$  [5].

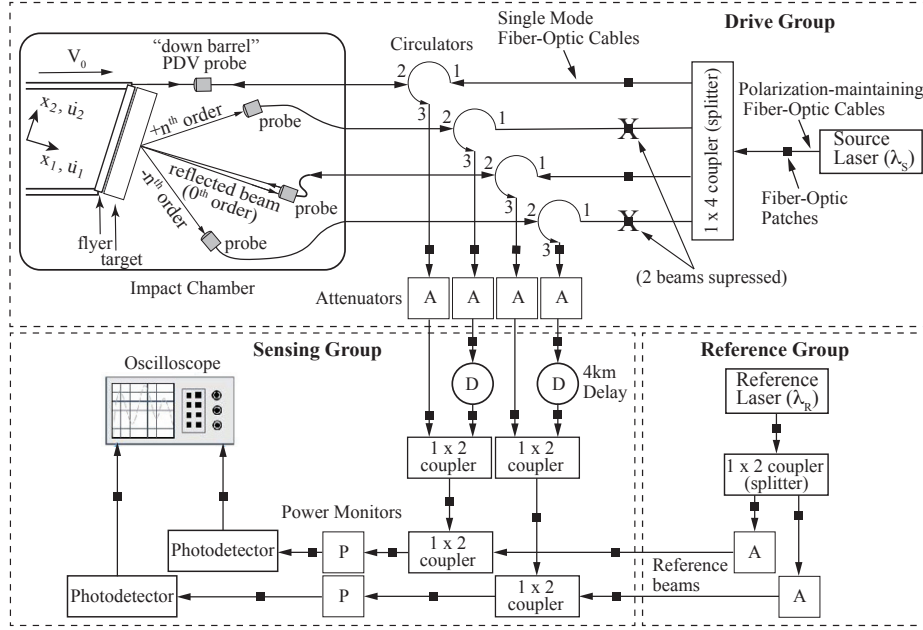


FIGURE 1. DPDV system for combined measurement of normal and transverse particle velocities in PSPI experiments

## DPDV FIBER-OPTIC CONFIGURATION

The fiber-optic DPDV arrangement is comprised of the drive, reference, and sensing groups as depicted in Fig. 1. The source light is produced by a KOHERAS BOOSTIK model E15 fiber laser by NKT Photonics with a Lorentzian linewidth of 0.1kHz (which translates to a very long coherence length), adjustable center wavelength between 1550 nm and 1570 nm, and a maximum output power of 2W. The drive group hardware elements include a  $1 \times 4$  fiber-optic splitter, fiber-optic circulators, attenuators, and fiber-optic probes. The “down barrel” probe is a collimating PDV probe which collects normally scattered light from the roughened surface of the sabot. The center probe adjacent to the target rear surface produces an incident,  $\approx 0.3$  mm diameter, collimated beam and collects the  $0^{th}$  order (collimated) beam reflected from the rear surface of the target. Symmetrically diffracted (collimated)  $\pm 1^{st}$  order beams are received by pigtail style collimators with an  $f=6.2$  mm aspheric lens with a 5 mm clear aperture. All four light beams are directed back toward their respective circulators which re-direct the light through SM fiber and FC/APCs to Variable Fiber Optic Attenuators as depicted in Fig 1. Each of the four collected light beams is passed through a fiber-optic circulator and redirected to variable fiber-optic attenuators before propagating to the sensing group elements as depicted in Fig. 1.

Reference group hardware elements depicted in Fig. 1 generate the reference beams, which are interfered with the four collected drive group source beams. The reference light is produced by a KOHERAS ADJUSTIK fiber laser by NKT Photonics, with a Lorentzian linewidth of 0.1kHz, adjustable center wavelength between 1535 nm and 1580 nm and a maximum power output of 40 mW. A reference beam wavelength of 1550.017 nm was selected for the validation experiment, which generated a constant carrier signal frequency of 0.66 GHz at zero particle velocity when mixed with the source light with a wavelength of 1550.012 nm.

Sensing group hardware elements depicted in Fig. 1 interfere the collected source light with the reference light and convert the resulting interference signals into digitized fringe records for analysis. The four Drive Group source beams are combined into PDV/DPDV beam pairs using two  $1 \times 2$  Single Mode (SM) fiber-optic couplers as shown. The diffracted light beams are each initially sent through a 4 km  $\times 2$  Network Simulation Module, which delays each beam by  $\approx 20 \mu\text{s}$  with respect to its PDV counterpart before the beams are combined. Each DPDV/PDV beam pair is then combined with a reference beam using a  $1 \times 2$  SM fiber-optic coupler with a 10/90 coupling ratio. Interfering beam trains terminate at a Photodetector where the modulating light fields are converted into electrical signals. The time multiplexed PDV and DPDV fringe records are digitized at 20 GS/s and recorded using only 2-channels of a 4-channel oscilloscope with a 4 GHz analog bandwidth.

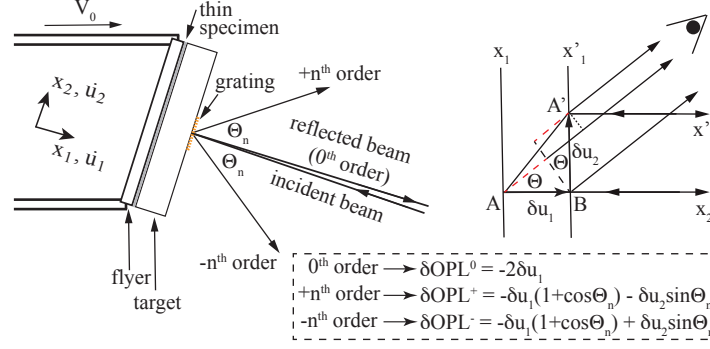


**FIGURE 2.** Changes in optical path length (OPL) of the 0<sup>th</sup> order (reflected) and  $\pm n^{\text{th}}$  order diffracted beams due to small (positive), normal and transverse displacements ( $\delta u_1, \delta u_2$ ) of the target rear surface as point A displaces to A'.

## INTERFEROMETER SENSITIVITY AND DATA ANALYSIS

DPDV measurement sensitivity is derived by invoking the two beam, time-averaged intensity formula

$$I \propto (\vec{E}_S + \vec{E}_R) \cdot (\vec{E}_S + \vec{E}_R)^* \quad (1)$$

where  $\vec{E}_S$  and  $\vec{E}_R$  are the electric field plane wave representations of the source and reference beams and the asterisk symbol denotes the complex conjugate operation [1, 6]. Substituting for all time varying phase terms including those corresponding to changes in optical path length (OPL) of the  $\pm n^{\text{th}}$  order diffracted beams, as shown in Fig. 2, leads to an expression for the time-averaged intensity of the heterodyned DPDV interference signals given by

$$I^\pm(t) = I_S^\pm + I_R^\pm + 2\sqrt{I_S^\pm I_R^\pm} \cos \left[ \frac{2\pi}{\lambda_S} (u_1(t)(1 - \cos \theta_n) \pm u_2(t) \sin \theta_n) + 2\pi(\nu_S - \nu_R)t - \phi^\pm \right]. \quad (2)$$

Here  $I_S$  and  $I_R$  represent the time-averaged steady state intensity of the source and reference beams,  $\lambda_S$  represents the wavelength of the source light,  $\nu_S$  and  $\nu_R$  are the optical frequencies of the source and reference light fields, and  $\phi^\pm$  is an arbitrary constant phase in each interference signal. Application of a moving-window discrete Fourier transform (DFT) algorithm to the recorded DPDV fringe records extracts the encoded signal frequencies corresponding to

$$f^+(t) = \frac{1}{\lambda_S} (\dot{u}_1(t)(1 + \cos \theta_n) + \dot{u}_2 \sin \theta_n) + (\nu_S - \nu_R) \quad (3)$$

$$f^-(t) = \frac{1}{\lambda_S} (\dot{u}_1(t)(1 + \cos \theta_n) - \dot{u}_2 \sin \theta_n) + (\nu_S - \nu_R) \quad (4)$$

where  $\dot{u}_1(t)$  and  $\dot{u}_2(t)$  correspond to the normal and transverse particle velocity components.

Subtracting the two DPDV signal frequencies given by Eqs. 3,4 and substituting for  $\sin \theta_n$  from the grating equation

$$d \sin \theta_n = n\lambda_S \quad n = \pm 1, 2, 3... \quad (5)$$

yields an expression for the transverse particle velocity in terms of the grating pitch ( $d$ ), diffraction order ( $n$ ), and the extracted signal frequencies given by

$$\dot{u}_2 = \frac{d}{2n} (f^+(t) - f^-(t)). \quad (6)$$

The frequency scaling factor  $d/2n$  effectively represents the fundamental measurement sensitivity of the DPDV to changes in transverse velocity and is equivalent to the sensitivity of a TDI [1]. Using the  $\pm 1^{\text{st}}$  order beams from a 400 lines/mm grating in the current DPDV configuration results in a transverse velocity measurement sensitivity of 1.25 m/s/MHz.

Addition of the two DPDV signal frequencies given by Eqs. 3 and 4 yields an expression for the normal particle velocity in terms of the measured signal frequencies and the independently measured carrier frequency ( $\nu_C = \nu_S - \nu_R$ )

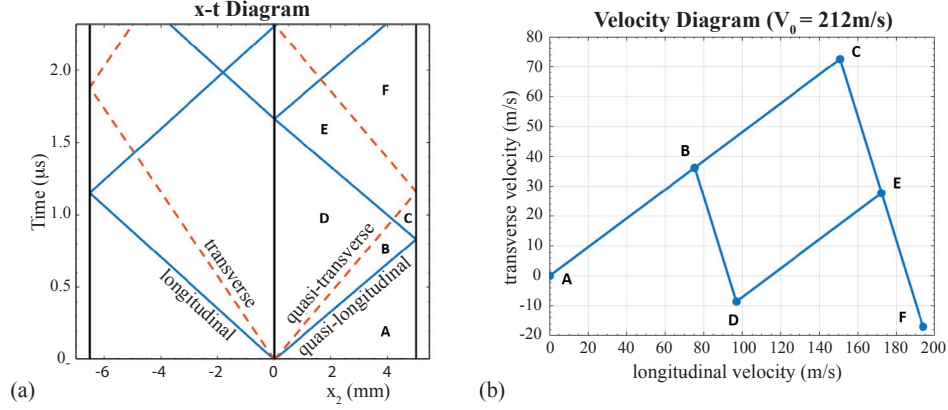


**FIGURE 3.** (a) x-t diagram displays wave characteristics in the flyer plate ( $-6.5 \text{ mm} \leq x_2 \leq 0 \text{ mm}$ ) and target plate ( $0 \text{ mm} \leq x_2 \leq 5 \text{ mm}$ ) (b) Predicted target plate particle velocities for an impact velocity of  $V_0 = 212 \text{ m/s}$  measured by the “down barrel” PDV

given by

$$\dot{u}_1 = \frac{\lambda_S}{2(1 + \cos \theta_n)} (f^+(t) + f^-(t) - 2v_C). \quad (7)$$

The scaling factor  $\lambda_S/(2(1 + \cos \theta_n))$  represents the fundamental measurement sensitivity of the DPDV to changes in normal velocity. DPDV is evidently  $(1 + \cos \theta_n) \times$  more sensitive to changes in normal velocity compared to a standard PDV, which has a sensitivity of  $\lambda_S/2$  [4]. Using the  $\pm 1^{\text{st}}$  order beams of a 400 lines/mm grating in the current DPDV configuration results in a normal velocity measurement sensitivity of 0.434 m/s/MHz, which represents a  $1.78 \times$  increase over the sensitivity of the PDV when using the  $0^{\text{th}}$  order beam at the same source wavelength.

## EXPERIMENTAL VALIDATION - NORMAL IMPACT OF Y-CUT $\alpha$ -QUARTZ

A normal plate impact experiment was conducted using a borosilicate glass flyer plate and a single crystalline y-cut  $\alpha$ -quartz target plate as a means of validating the new DPDV-PDV system. Single crystalline y-cut  $\alpha$ -quartz was selected as a target material because of the strong anisotropic coupling exhibited between longitudinal and transverse particle motion when impacted along its  $x_2$  axis. Quasi-longitudinal (QL) and quasi-transverse (QT) waves with wave speeds,  $c_{QL} = 6015.64 \text{ m/s}$ , and  $c_{QT} = 4318.39 \text{ m/s}$  emerge as the only nonzero eigenvalues of the elasto-acoustic tensor which governs the problem [1]. The sharp velocity jumps registered in the normal and transverse directions upon arrival of the QL and QT waves at the rear surface of the target present an ideal scenario for evaluating various attributes of the DPDV system such as predicted velocity measurement sensitivities and the optical heterodyne feature for automatic, accurate detection of sharp velocity reversals.

The x-t diagram in Fig. 3(a) depicts the QL and QT wave characteristics in the quartz target plate and the transverse and longitudinal wave characteristics in the isotropic, borosilicate flyer plate. Six unique states of constant particle velocity and stress are identified and labeled A - F in the x-t diagram. The particle velocity components for each state were computed based on an impact velocity of  $V_0 = 212 \text{ m/s}$  as measured by the “down barrel” PDV and plotted as coordinate pairs  $(\dot{u}_1, \dot{u}_2)$  in the velocity diagram in Fig. 3(b). Sharp step-like velocity jumps of  $\dot{u}_1^C = 150.79 \text{ m/s}$  and  $\dot{u}_2^C = 72.51 \text{ m/s}$  are predicted upon arrival of the QL wave at the rear surface of the target plate. The subsequent arrival of the QT wave induces a pronounced reversal of the transverse velocity from  $\dot{u}_2^C = 72.51 \text{ m/s}$  to  $\dot{u}_2^F = -17.02 \text{ m/s}$  and a second positive jump in the normal particle velocity from  $\dot{u}_1^C = 150.79 \text{ m/s}$  to  $\dot{u}_1^F = 193.84 \text{ m/s}$  corresponding to the path C  $\rightarrow$  F in the velocity diagram (Fig. 3(b)).

The choice of borosilicate for the flyer plate material was based on three considerations: (a) choice of an isotropic material to simplify material alignment requirements, (b) a low acoustic impedance to generate relatively low normal stresses in both plates, and (c) sufficiently high yield strength in compression and shear to prevent premature failure of the flyer plate. Cylindrical plates of Borofloat 33 glass were prepared with the following specifications: (a) diameter =  $33.909 \pm 0.1 \text{ mm}$ , (b) thickness =  $6.5 \pm 0.1 \text{ mm}$ , and (c) RMS surface roughness  $< 1 \text{ nm}$ . The borosilicate plate

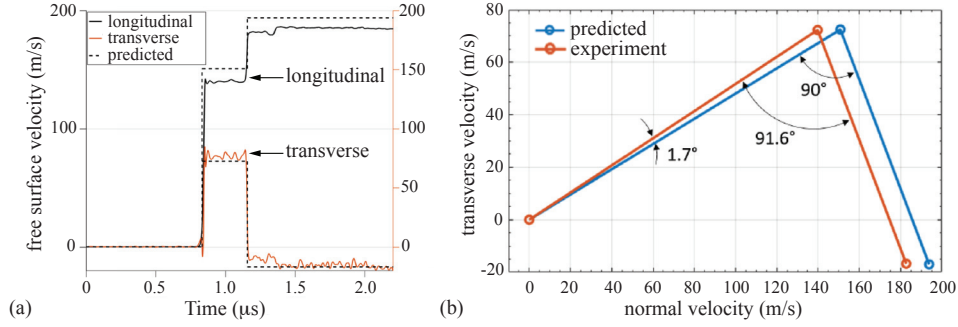


**FIGURE 4.** (a) Measured longitudinal and transverse velocity profiles compared to predicted values based on the measured impact speed of  $V_0 = 212$  m/s (b) Orthogonality of the measured velocity jumps during the arrival of the QL wave, and later the QT wave

thickness was chosen to prevent wave reflections from the backside of the flyer plate from reaching the impact face before separation. Values for borosilicate material constants were obtained from Schott North America and are given as given as follows: (a) density  $\rho = 2.23$  g/cm<sup>3</sup>, (b) elastic modulus  $E = 64$  GPa, (c) Poisson's ratio  $\nu = 0.2$ .

Cylindrical y-cut  $\alpha$ -quartz plates were prepared with the following specifications: (a) diameter =  $30 \pm 0.1$  mm, (b) thickness = 5 mm, and (c) RMS surface roughness of  $8 - 10$  Å. The target plate diameter provided an observation window of more than  $2 \mu\text{s}$  before lateral release waves from the plate boundary reached the center of the target. The z-axis of the y-cut substrate was found using a petrographic microscope and interference figures and marked with an etched line on the plate's circumference. Values for density and elastic-acoustic tensor constants were obtained from literature and are given as follows: (a) density  $\rho = 2.65$  g/cm<sup>3</sup>, (b)  $C_{22} = 87.16$  GPa, (c)  $C_{24} = 18.15$  GPa, (d)  $C_{44} = 58.14$  GPa, (e)  $C_{66} = 40.26$  GPa.

A 300 nm thick gold diffraction grating was fabricated onto the backside of the polished y-cut  $\alpha$ -quartz target plate using standard photolithography procedures and metal vapor deposition techniques in a cleanroom environment. A 400 lines/mm ( $d = 2.5 \mu\text{m}$ ) diffraction grating was produced with its grating lines aligned parallel to the  $x_1$ -axis of the y-cut quartz substrate. The grating thus produces sharp, specular 0<sup>th</sup> order and  $\pm 1^{\text{st}}$  order diffraction beams along precisely known diffraction angles  $\theta_{\pm 1} = \pm 38.32^\circ$  per Eq. 5. No additional diffraction orders are produced by the 400 lines/mm grating at the source wavelength ( $\lambda = 1550$  nm) used in the current DPDV system. DPDV probes are aligned to the  $\pm 1^{\text{st}}$  order diffraction angles by optimizing the light return from each diffracted beam until the maximum light returns are achieved.

Normal and transverse velocity profiles measured at the rear surface of the y-cut  $\alpha$ -quartz target plate using the DPDV system are plotted in Fig. 4(a). The velocity profiles were obtained from the acquired fringe records using a Hamming window of 50 ns with the window shifted by a 50 ps time step for every analysis. The dashed lines represent the predicted velocity jumps of each respective motion component. The measured steady initial and final transverse particle velocity levels are in excellent agreement with theory while the measured normal velocity jumps are within 6 – 7% of their respective predicted values. The observed deviation is attributed to a small tilt angle  $\phi \approx 1$  mrad between impact faces, which causes the QL wave to deviate from the  $x_2$  axis (quartz crystal y-axis) by an amount consistent with the observed deviation. The observed deviation is also be partly attributed to uncertainties in the values of the elastic constants for  $\alpha$ -cut quartz and borosilicate glass.

Since the target plate's free surface velocity is proportional to the orthogonal QL and QT wave polarization vectors, the transient velocity jump is ideally orthogonal to the final velocity jump as depicted Fig. 4(b). The measured velocity jumps during the arrival of the QL wave, and later the QT wave, show a slight deviation from predicted values. Specifically, the QL wave's polarization deviated by  $1.7^\circ$  and the QT wave's polarization deviated by  $0.1^\circ$ . Measured values are respectively quite comparable and even slightly lower than the jump offsets of  $2.15^\circ$  and  $1.7^\circ$  reported by [1] in their original TDI validation experiments on y-cut quartz which had a measured impact tilt angle of 0.4 mrad.

## ACKNOWLEDGMENTS

The authors are grateful for support from the Office of Naval Research (Award No. N00014-16-1-2839) for the development of the PSPI capability at high pressures and the Air Force Office of Scientific Research (Award No. FA9550-12-1-0091) for the development of the heterodyne diffracted beam photonic Doppler velocimeter (DPDV) system.

## REFERENCES

- [1] K. Kim, R. Clifton, and P. Kumar, *J. Appl. Phys.* **48,10**, 4132–4139 (1977).
- [2] L. Chhabildas, H. Sutherland, and J. Asay, *J. Appl. Phys.* **50,8**, 5196–5201 (1979).
- [3] B. Zuanetti, T. Wang, and V. Prakash, *Rev. Sci. Instrum.* **88, 3**, p. 033108 (2017).
- [4] D. Dolan, *Rev. Sci. Instrum.* **81,5**, p. 053905 (2010).
- [5] C. Kettenbeil, M. Mello, T. Jiao, R. Clifton, and G. Ravichandran, in *Shock Compression of Condensed Matter - 2017*, edited by R. Chau, T. Germann, and M. Lane. (American Institute of Physics, Melville NY, 2018).
- [6] H. Espinosa, M. Mello, and Y. Xu, *J. Appl. Mech.* **64,1**, 123–131 (1997).